Oscillatory and resonant effects at the boundary in a bicrystal of an anisotropic metal

S. N. Burmistrov and L. B. Dubovskiĭ

I. V. Kurchatov Institute of Atomic Energy, Moscow

A classification is given of the possible types of motion of an electron at the internal boundary in a bicrystal subjected to a magnetic field. The discrete spectrum of electron states obtained for this boundary is specific to each type of bicrystal and it gives rise to oscillatory and resonant effects characteristic of the bicrystal type. The experimental pattern of these effects can be deduced from the nature of the transition layer in a bicrystal.

1. INTRODUCTION

Bicrystals, perfect junctions of two single crystals are attracting much interest. Bicrystals exhibit anomalies of various physical properties at the internal boundary and these anomalies do not occur in the case of the individual single crystals.[1-3] The effects observed experimentally are of integral nature and therefore a clear microscopic treatment of these effects is lacking. One of the possible reasons for the anomalies at the internal boundary is the change in the lattice properties and in the phonon spectra at this boundary. An alternative microscopic cause of these anomalies is a modification of the electron spectrum that occurs near the internal boundary in a bicrystal. High-resolution electron microscopy[4] has demonstrated that the internal boundary in a bicrystal is coherent at the atomic level. In particular[5] the layer system $YBa_2CuO_{7-\delta}$ with the orthorhombic phase, in which the cubic lattice of the perovskite is distorted, readily forms twins. The twinning law can easily be explained on the basis of the point symmetry of a crystal assuming that twinning of this system represents a transition from the tetragonal phase in the course of cooling. The twin boundaries are coherent in the (110) plane. Twinning at the boundary results in transposition of the periods along the crystallographic axes a and b in the basal plane and a transition of this kind occurs without the formation of a kink of Cu atoms across a twinning plane.

The characteristic features of the behavior of electrons at a grain boundary was considered by Kaganov and Fiks[6] for an anisotropic dispersion law in the case of specularly and diffusely reflecting boundaries. Passage of an electron wave across a specularly reflecting boundary is accompanied by refraction and reflection that obey the laws of conservation of energy and of conservation of the tangential component of the quasimomentum. In the case of an anisotropic Fermi surface there are electrons which undergo total internal reflection similar to the corresponding effect in optics and associated with the fact that both laws of conservation cannot be satisfied simultaneously. Such a feature of the passage of electrons across a boundary gives rise to various anomalies such as the appearance of electromechanical forces created by an electric current and concentrated near the boundary,[6] a specific dependence of the resistance of a bicrystal on the angle of misorientation of the single crystals,[7] and a special behavior of the whole system in a magnetic field as well as existence of discrete electron states at the twinning boundary.[8]

The boundary conditions that ensure conservation of energy and of the tangential component of the quasimomentum give rise to an effective potential in which an electron is moving. In Sec. 2 we shall classify possible types of motion in such an effective potential.

In Sec. 3 we shall consider the characteristic features of the behavior of a bicrystal of general type in a magnetic field parallel to the internal boundary. The total internal reflection effect and the corresponding effective potential cause some of the electrons moving near the boundary not to follow a circular path as in the bulk of a bicrystal but jump-like paths involving a reflection from the boundary (Fig. 1a) or along paths in the form of an asymmetric lens when the boundary is crossed (Fig. 1b). The jump-like paths induce magnetic surface levels, exactly as in the familiar case of a specularly reflecting surface of a metal.[9] However, there is an important difference between a specularly reflecting surface of a metal and the internal boundary in a bicrystal, because such surface levels have a specific geometric orbit along which the frequency of classical motion of an electron changes abruptly. The abrupt change in the frequency is due to the fact that the motion of an electron in a magnetic field near a twinning boundary occurs in a two-well potential (Fig. 2). We shall show in Sec. 4 that this gives rise to a new period of quantum oscillations different from the period of oscillations in the bulk of a metal.

In Secs. 5 and 6 we shall consider two types of levels on a twinning plane. The first represents discrete states which appear in a symmetric potential well in the absence of a magnetic field. The second appears due to the splitting of levels in a symmetric two-well potential that occurs when a magnetic field is parallel to the boundary and the effective kinematic potential acts as a barrier.

We shall conclude this introductory section by noting that all the various effects described above are associated
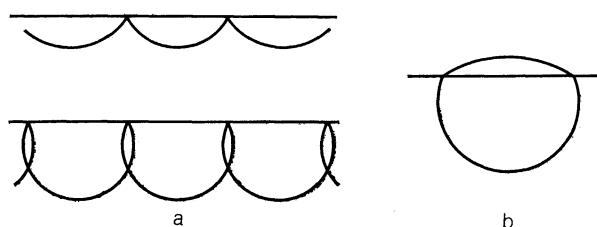

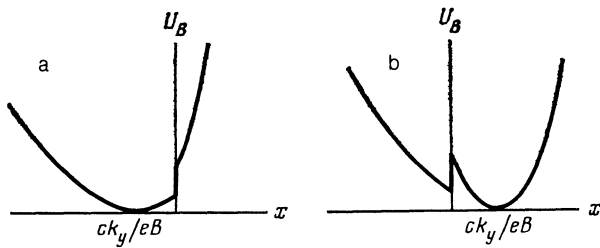FIG. 1. Electron paths in a magnetic field.

0038-5646/88/091831-11$04.00

FIG. 2. Effective potential U_B for a bicrystal in a magnetic field shown for the quasimomenta $k_y < 0$ (a) and $k_y > 0$ (b).

primarily with the fact that the internal coherent boundary in a bicrystal differs from a specularly reflecting surface of a metal. This difference consists in the fact that a new type of symmetry appears in the case of the internal boundary in a bicrystal and this symmetry is associated with rotation of the Fermi surface in space as we go over from one single crystal to another, which does not occur in the case of a specularly reflecting metal surface.

2. CLASSIFICATION OF THE NATURE OF ELECTRON MOTION AT THE INTERNAL BOUNDARY IN A BICRYSTAL

The internal boundary in a bicrystal separates two physically identical phases differing only in respect of the orientations of the crystallographic axes in space. In the case of an isotropic electron spectrum ($\varepsilon = \mathbf{p}^2/2m$) there are no special features due to the passage of electrons across such a boundary. The situation changes radically if the electron spectrum is anisotropic. As pointed out in the Introduction, in this case some of the electrons are reflected at the boundary because the laws of conservation of energy and of the tangential component of the quasimomentum cannot be satisfied in the other parts of the bicrystal. Consequently, an effective kinematic potential appears at the boundary and an electron moves in this potential.

The dependence of the electron energy ε on the quasimomentum $\mathbf{p}$ will be selected, for the sake of simplicity, as simple as possible but yet representing the anisotropy of a metal. This requirement is satisfied by a quadratic anisotropic dispersion law with the masses m_1, m_2, and m_3 along the principal crystallographic axes. We shall assume that x is the coordinate along the normal to the surface of a bicrystal and that the principal crystallographic axes 1 and 2 are rotated by an angle $\varphi = \varphi(x)$ relative to the spatial axes x and y. The Hamiltonian then becomes

$$\hat{H} = -\frac{1}{2}\frac{\partial}{\partial x}\left(\frac{1}{m_{11}(x)}\frac{\partial}{\partial x}\right)$$
$$-\frac{1}{2}\left[\frac{\partial}{\partial x}\left(\frac{1}{m_{12}(x)}\right)+\frac{1}{m_{12}(x)}\frac{\partial}{\partial x}\right]$$
$$-\frac{1}{2m_{22}}\frac{\partial^2}{\partial y^2}-\frac{1}{2m_3}\frac{\partial^2}{\partial z^2}. \quad (1)$$

Elements of the mass tensor m_{ik}^{-1} can then be expressed as follows in terms of m_1, m_2, and m_3:

$$\begin{pmatrix} m_{11}^{-1} & m_{12}^{-1} \\ m_{21}^{-1} & m_{22}^{-1} \end{pmatrix}$$
$$=\begin{pmatrix} m_1^{-1}\cos^2\varphi+m_2^{-1}\sin^2\varphi, & (m_1^{-1}-m_2^{-1})\sin\varphi\cos\varphi \\ (m_1^{-1}-m_2^{-1})\sin\varphi\cos\varphi, & m_1^{-1}\sin^2\varphi+m_2^{-1}\cos^2\varphi \end{pmatrix}. \quad (2)$$

The angle $\varphi(x)$ varies smoothly at the boundary of a bicrystal from the value φ_- in the left-hand half-space to φ_+ in the right-hand space $[\varphi_- \leqslant \varphi(x) \leqslant \varphi_+]$ over a distance L representing modification of the crystallographic axes near the internal boundary of a bicrystal due to a change from one single crystal to another.

The adopted form of Eq. (1) ensures that the Hamiltonian is Hermitian for an arbitrary dependence of the angle of rotation φ on the coordinate x. If $L \gg a_0$, where a_0 is the interatomic distance, then in the transition layer between the two single crystals as well as in the rest of the bicrystal we can use the effective mass approximation in the Hamiltonian of Eq. (1). The condition $L \gg a_0$ and the requirement that the Hamiltonian should be Hermitian determine uniquely the form of Eq. (1) as the Hamiltonian with a constant mass $m_{ik}(\varphi)$ of Eq. (2) for a fixed angle of rotation φ. It is shown in Ref. 10 (§ 8) that, in general, the requirements of the Hermitian behavior used in the semiclassical approach defines uniquely the Hamiltonian on the basis of its classical analog. If $L \sim a_0$, the Hamiltonian in form (1) is already model-like: interband transitions are deliberately ignored and, what is more important, so are the Bloch modulations of the electron wave. Therefore, the analysis is in fact carried out not for Bloch electrons but for their envelopes and this corresponds exactly to an approximation with the effective mass in one band. However, the approximation represented by Eq. (1) is quite satisfactory in the case of a wide range of problems. This applies particularly to the behavior of a system in a magnetic field when the size $r_B = cp_F/eV$ of an electron orbit in a field is much greater than the interatomic distance, so that the thickness of the transition layer between the two single crystals becomes unimportant. Another characteristic example is the class of semimetals in which the electron wavelength λ is much greater than a_0 and L is again unimportant. In the case of real bicrystals[4,5] the value of L is usually $(3$–$4)a_0$. The dependence of the electron spectrum on the distance from a metal-vacuum interface has been investigated already.[11] Calculations demonstrate that in this case the characteristic scale or distance in which the spectrum changes amounts to several interatomic spacings. For a bicrystal internal boundary the transition layer is also at least several interatomic spacings thick.

In the investigation of the energy spectrum of the Hamiltonian (1) we shall use the Fourier components along the coordinates y and z parallel to the internal surface in a bicrystal and we shall then perform a scaling transformation of the wave-function phase $\psi(x)$:

$$\psi(x)=\bar{\psi}(x)\exp\left\{-ik_y\int_0^x dx'\, m_{11}(x')/m_{12}(x')\right\}.$$

Then, the Hamiltonian of Eq. (1) becomes

$$\hat{H} = -\frac{1}{2}\frac{d}{dx}\left(\frac{1}{m_{11}(x)}\frac{d}{dx}\right)+\frac{1}{2}\frac{m_{11}(x)}{m_1 m_2}k_y^2+\frac{1}{2m_3}k_z^2; \quad (3)$$

k_y and k_z are the conserved components of the quasimomentum along the bicrystal boundary. The components of the mass tensor along the x, y, and z axes are m_x, m_y, and m_z, respectively, and their values are given by

$$m_x=m_{11}(x), \quad m_y=m_1 m_2/m_{11}(x), \quad m_z=m_3. \quad (4)$$

The term with a kinetic energy $K(x) = k_y^2/2m_y(x)$ and a

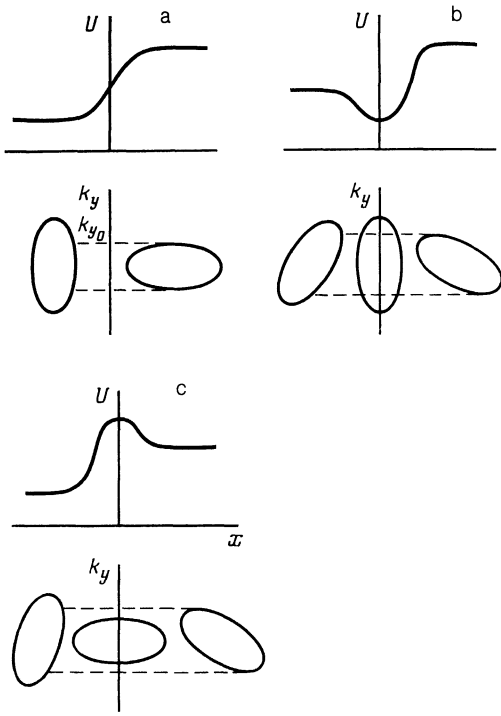S. N. Burmistrov and L. B. Dubovskiĭ   1832

FIG. 3. Possible types of the potential U at the boundary and the corresponding orientations of the equal-energy surfaces in different parts of a bicrystal.

variable mass $m_y(x)$ represents the effective potential energy $U(x)$ in the field of which an electron is moving.

Figure 3 shows typical $U(x)$ dependences applying to a general bicrystal plotted as functions of the relative orientations of the crystallographic axes in the two single crystals. The simplest situation is shown in Fig. 3a. In this case if the electron momentum in the left-hand half-space exceeds k_{y0} ($|k_y| > k_{y0}$), then such an electron cannot penetrate into the right-hand half-space because in this space there is no state with a momentum ensuring conservation of the electron energy and of the components of the momentum k_y and k_z along the internal bicrystal boundary. Therefore, a potential barrier appears at the boundary and this barrier is associated with the kinematics of the motion of an electron at the bicrystal boundary and it is analogous to the centrifugal energy in a centrally symmetric field. Figure 3b illustrates the case when the mass ellipsoid rotates all the time in the positive direction of the angle φ (i.e., it rotates anticlockwise). Then, at the boundary we shall in turn have twice the situation corresponding to Fig. 3a, first when the electron crosses from the right to left and then from the left to right. Consequently, a potential well with generally asymmetric edges appears in the transition region at the boundary. In Fig. 3c the effective mass ellipsoid rotates in the opposite direction, i.e., clockwise. Then, we again have two repetitions of the situation in Fig. 3a, but in the opposite sequence and this gives rise to a potential barrier.

It therefore follows that, for a given position of the mass ellipsoid both at $+\infty$ and $-\infty$ characterized by φ_- and φ_+, we can have internal boundaries in a bicrystal which are completely different from the point of view of the electron spectrum (Fig. 3). The variety of possible situations is not limited to the cases just discussed. There is an additional discrete parameter l which labels all possible types of the bicrystal boundary. This parameter l characterizes the total change in the angle φ on passage from one single crystal to the other in a bicrystal described by

$$\Delta\varphi = \varphi_+ - \varphi_- + \pi l, \quad l = 0, \pm 1, \pm 2, \pm 3, \ldots. \tag{5}$$

The number l represents the number of extrema of the effective potential energy $U(x)$. The change in l by unity gives rise or suppresses an additional well-barrier pair in the relief of the effective potential $U(x)$. The sign of l determines the sequence of the potential barrier and the well. Bicrystals usually studied experimentally are clearly characterized by the minimum number of extrema of the function $U(x)$. However, specially grown bicrystals can in principle have any value of l.

A special symmetry is exhibited by a twin crystal characterized by

$$\varphi_+ = -\varphi_- = \varphi_0. \tag{6}$$

Then, for a given value of φ_0 we have two possibilities: a symmetric barrier or a symmetric potential well (Figs. 4b and 4a). In the latter case[8] there is at least one bound level.

This situation may occur not only in crystals with a complex anisotropic lattice, but also in cubic crystals. It is essential however that the Fermi surfaces should not become superimposed exactly on one another as a result of a homogeneous spatial displacement from one single crystal to the other. Since in the case of cubic crystals the quadratic dispersion law is always isotropic, the effects under consideration can occur only in crystals with a nonquadratic dispersion law. The most suitable crystals are metals with the Fermi surface either intersecting the boundaries of the Brillouin zone or approaching closely these boundaries, in the case of Nb (Ref. 2). Complex dispersion laws can be discussed in a similar manner. We shall simply point out here that in the case of complex Fermi surfaces there may be effects associated with the birefringence of an electron wave[10] crossing the boundary of a bicrystal.

We have considered above a tilt boundary in a bicrystal[7] when the rotation of the axes of the Fermi surface occurs in one plane. In the case of a twist boundary, when the crystallographic axes are rotated in three dimensions, we may have a potential well or a barrier depending on the direction in (k_y, k_z) quasimomentum plane.

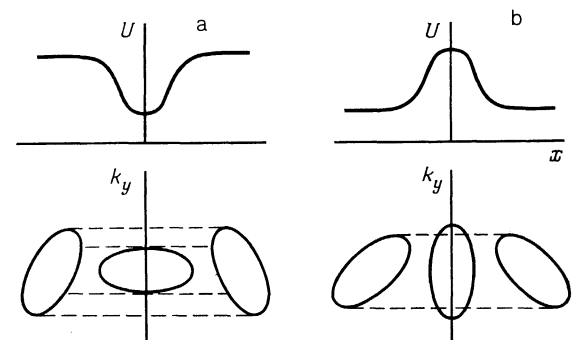We shall consider the simplest situations corresponding to Figs. 3a, 4a, and 4b.

FIG. 4. Possible types of the potential U at a twinning boundary and the corresponding changes of the equal-energy surfaces in space.

3. SYSTEMATICS OF MAGNETIC DISCRETE LEVELS AT THE BOUNDARY IN A BICRYSTAL

An effective potential in the form of a step (Fig. 3a) appears at the boundary of a general type in a bicrystal. This potential has a strong influence on the behavior of electrons in a magnetic field parallel to the boundary. This is due to the fact that some of the conduction electrons move in a magnetic field along jump-like orbits (Fig. 1), which is an effect well known for a specularly reflecting surface of a metal and results in the appearance of magnetic surface levels. As a consequence, a system of this kind exhibits Khaĭkin oscillations of the surface impedance in a weak magnetic field, when the impedance is plotted as a function of the field or frequency,[9] and this applies to a large number of metals (Sn, In, Cd, Al, W, Bi, Ga) which have a nonquadratic spectrum. However, at the boundary in a bicrystal there are some special features not observed for a specularly reflecting metal surface. This is due to the fact that among the electrons colliding with a specularly reflecting surface there are none with orbits special in the geometric sense and, therefore, electrons incident on a specularly reflecting surface do not contribute to oscillations of the magnetic susceptibility.[12] However, at the internal boundary in a bicrystal there are electrons crossing this boundary and forming a geometrically special orbit, giving rise to a new period of quantum oscillations of the magnetic susceptibility.

The description of the motion of electrons in a homogeneous magnetic field parallel to the internal boundary in a bicrystal is analogous to that given by Eqs. (1)–(3):

$$\hat{H} = -\frac{1}{2}\frac{\partial}{\partial x}\left(\frac{1}{m_{11}(x)}\frac{\partial}{\partial x}\right) - \frac{1}{2}\frac{m_{11}(x)}{m_1 m_2}\left(\frac{\partial}{\partial y} - i\frac{e}{c}A_y(x)\right)^2$$
$$- \frac{1}{2m_3}\left(\frac{\partial}{\partial z} - i\frac{e}{c}A_z(x)\right)^2. \tag{7}$$

The vector potential $\mathbf{A}$ can be expressed as follows in terms of the magnetic induction vector $\mathbf{B}(x) = [0, B_y(x), B_z(x)]$:

$$A(x) = \left(0, \int_0^x dx' B_z(x'), -\int_0^x dx' B_y(x')\right).$$

If we now go over to the Fourier components along the y and z axes, we obtain the following one-dimensional potential $U_B(x)$ for the motion of an electron and this potential depends on the components of the momentum along the boundary:

$$U_B(x) = \frac{1}{2}\frac{m_{11}(x)}{m_1 m_2}\left[k_y - \frac{e}{c}A_y(x)\right]^2$$
$$+ \frac{1}{2m_3}\left[k_z - \frac{e}{c}A_z(x)\right]^2. \tag{8}$$

The situation simplifies greatly if the magnetic field is parallel to the z axis. We then have $A_z(x) \equiv 0$ and the energy of motion can be divided into two terms each of which depends only on one component of the momentum:

$$E(k_y, k_z) = \varepsilon(k_y) + \frac{k_z^2}{2m_3}. \tag{9}$$

When the motion of an electron in a magnetic field is

considered, it is possible to ignore the distance L representing the change in the orientation of the crystallographic axes from one single crystal to another near the internal boundary in a bicrystal, because the radius of the electron orbit r_B is large compared with the thickness L of the transition layer. In this case we can assume that $m_{11}(x) = m_1\theta(-x) + m_2\theta(x)$ $(m_2 > m_1)$, which corresponds to a distribution $\varphi(x) = (\pi/2)\theta(x)$. In the case of a homogeneous distribution $A_y(x) = Bx$ the effective potential is

$$U_B(x) = \frac{1}{2}\frac{m_{11}(x)}{m_1 m_2}\left(k_y - \frac{e}{c}Bx\right)^2, \tag{10}$$

which depends strongly on the sign of k_y (Fig. 2). If $k_y > 0$, we have a two-well potential with two different frequencies of the classical motion. It is convenient to split the description of the energy spectrum into three regions in accordance with the energy ε of Eq. (9):

$$0 < \varepsilon < k_y^2/2m_2, \tag{11a}$$

$$k_y^2/2m_2 < \varepsilon < k_y^2/2m_1, \tag{11b}$$

$$\varepsilon > k_y^2/2m_1. \tag{11c}$$

In the region of Eq. (11a) the classical motion occurs along a circle located at $x > 0$. In the range of energies defined by Eq. (11b) there are two types of path: a circle at $x > 0$ and jump-like paths when $x < 0$ (Fig. 1a). In the range defined by Eq. (11c) a more complex path has the shape of an asymmetric lens representing two arcs of a circle joined together (Fig. 1b). The values of the energy ε are, respectively, 0, $k_y^2/2m_2$, and $k_y^2/2m_1$, which represent singularities of the spectrum where the classical motion frequency undergoes a jump and the density of states has an anomaly. If $k_y < 0$ (Fig. 2a), there are also singularities of the spectrum at these points.

A description of the energy spectrum throughout the full range of parameters can be semiclassical. We shall adopt such a description for the most interesting part of the spectrum defined by Eq. (11b) and representing jump-like paths $(k_y > 0)$. The wave function in the classically attainable region $-a < x < 0$ is

$$\psi(x) = A p^{-1/2}\cos\left(\int_{-a}^x p\,dx - \pi/4\right), \tag{12}$$

$$p = \left\{2m_1\left[\varepsilon - \frac{1}{2m_2}\left(k_y - \frac{eB}{c}x\right)^2\right]\right\}^{1/2},$$

$$a = \frac{ck_y}{eB}\left[(1+\xi)^{1/2} - 1\right].$$

Here, the quantity ξ determines the spectrum as follows:

$$\varepsilon = \frac{k_y^2}{2m_2}(1+\xi). \tag{13}$$

In the part of the spectrum under consideration the value of ξ lies within an interval corresponding to Eq. (11b):

$$0 < \xi < \rho, \tag{13a}$$

where ρ represents the anisotropy of the spectrum: $\rho = (m_2 - m_1)/m_1$. If $x > 0$, the wave function decays with depth in the metal:

S. N. Burmistrov and L. B. Dubovskiĭ   1834

$$\psi(x) = Bq^{-1/2}(x)\exp\left(-\int_0^x q(x')\,dx'\right),$$

$$q(x) = \left\{2m_2\left[\left(k_y - \frac{eB}{c}x\right)^2 \middle/ 2m_1 - \varepsilon\right]\right\}^{1/2}. \quad (14)$$

The function $\psi(x)$ and its first derivative $\psi'(x)$ are continuous at the point $x = 0$:

$$Ap^{-1/2}(0)\cos\left(\int_{-a}^0 p\,dx - \pi/4\right) = Bq^{-1/2}(0),$$

$$Ap^{1/2}(0)\sin\left(\int_{-a}^0 p\,dx - \pi/4\right) = Bq^{1/2}(0).$$

This leads to the following quantization rule:

$$\int_{-a}^0 dx\left\{2m_1\left[\varepsilon_n - \frac{1}{2m_2}\left(k_y - \frac{eB}{c}x\right)^2\right]\right\}^{1/2} = \pi(n+\gamma_n),$$

$$\gamma_n = \frac{3}{4} - \frac{1}{\pi}\arctan\left(\frac{m_1}{m_2}\frac{\xi_n}{\rho - \xi_n}\right)^{1/2}.$$

Hence, we obtain the following expression for the spectrum:

$$\varepsilon_n = \frac{k_y^2}{2m_2}(1 + \xi_n), \quad (15)$$

where ξ_n is deduced from the relationship

$$n + \gamma_n = Q(\xi_n)k_y^2,$$

$$Q(\xi) = \frac{c}{\pi eB}(m_1/m_2)^{1/2}(1+\xi)$$

$$\times \left\{\arctan\left[\frac{\xi^{1/2}}{1+(1+\xi)^{1/2}}\right] - \frac{\xi^{1/2}}{2(1+\xi)}\right\}. \quad (15a)$$

In the limit of weak anisotropy ($\rho \ll 1$), we have

$$Q(\xi) = \frac{c}{eB}(m_1/m_2)^{1/2}(3\pi)^{-1}\xi^{3/2}.$$

The spectrum described by Eq. (15) is derived using the wave function such that only the decaying component is allowed for in the classically forbidden region of Eq. (14) and the growing component is disregarded. This corresponds to neglect of the influence of the second potential well in the range $x > 0$ (Fig. 2) on the spectrum of the first well. An allowance for this influence gives rise to exponentially small corrections relating to the overlap of the wells, which will be ignored.

An analysis of the spectrum in the remaining ranges defined by Eq. (11) can also be carried out semiclassically for $k_y > 0$ and $k_y < 0$. In the range defined by Eq. (11a) when $k_y < 0$ the motion occurs in the oscillator potential $U_B(x)$ (Fig. 2) and the momentum is

$$p(x) = \left\{2m_1\left(\varepsilon - \left(k_y - \frac{e}{c}Bx\right)^2 \middle/ 2m_2\right)\right\}^{1/2}, \quad x < 0.$$

Therefore, the motion is quantized in the usual way and we have

$$\varepsilon_n = \frac{eB}{c}(m_1 m_2)^{-1/2}(n + 1/2). \quad (16)$$

The corrections to this spectrum due to the jump of the potential at $x = 0$ are exponentially small, exactly as in the case corresponding to Eq. (15). Precisely the same spectrum (16) is obtained also for an oscillator well when $k_y > 0$ and $x > 0$ in the energy range defined by $0 < \varepsilon < k_y^2/2m_1$ corresponding to Eqs. (11a) and (11b). We can similarly consider the spectrum for the other regions defined by Eq. (11) which correspond to paths in the form of an asymmetric lens (Fig. 1b).

In the case of a more general potential $U_B(x)$ of Eq. (8), when a magnetic field is directed in the yz plane in an arbitrary manner, we can again use the semiclassical description:

$$\int dx\left\{2m_{11}(x)\left[E_n - \frac{1}{2}\frac{m_{11}(x)}{m_1 m_2}\left(k_y - \frac{e}{c}A_y(x)\right)^2\right.\right.$$
$$\left.\left. - \frac{1}{2m_3}\left(k_z - \frac{e}{c}A_z(x)\right)^2\right]\right\}^{1/2} = \pi(n+\gamma_n).$$

Integration in the above equation is carried out in the classically attainable region. The potential $U_B(x)$ at the point $x = 0$ undergoes a jump of magnitude $\rho k_y^2/2m_2$ and this generally creates a two-well potential when $k_y > 0$ and a potential with a jump when $k_y < 0$, similarly to the case illustrated in Fig. 2 and representing the special type of the potential discussed above.

4. OSCILLATIONS OF THE STATIC SUSCEPTIBILITY AT THE BOUNDARY IN A BICRYSTAL

We shall analyze oscillations of the static susceptibility by considering the expression for the microscopic density of the current $j_y(x)$ employing the Matsubara technique[13] which, after summation over the frequencies, gives

$$j(x) = \frac{2e}{m_y}\int\frac{dk_y\,dk_z}{(2\pi)^2}\left(k_y - \frac{e}{c}A_y\right)$$

$$\times \sum_n \psi_n^2(x)/[1 + \exp(E_n(k_y k_z) - \mu)/T]. \quad (17)$$

For simplicity, we shall confine our attention to the case of a weak anisotropy described by $\rho \ll 1$. The square of the wave function of Eq. (12) can be represented by a sum of two terms: one which varies continuously, $\frac{1}{2}[a(a+x)]^{1/2}$ and the other which oscillates rapidly as the coordinate x is varied. We shall be interested only in the smooth part of $j_y(x)$. At $x = 0$ this part can be represented in the form

$$j_v(0) = \frac{2e}{m}\int_0^\infty J(E)\,dE/[1 + \exp(E - \mu)/T],$$
$$\quad (18)$$
$$J(E) = \frac{1}{(2\pi)^2}\int_{-\infty}^{+\infty}dk_z\int_0^\infty k_y\,dk_y\sum_n\frac{1}{2a}\delta(E - E_n(k_y k_z)).$$

The summation over n can be carried out using the Poisson rule:

$$J(E) = J_0(E) + 2\,\mathrm{Re}\sum_{k=1}^\infty J_k(E),$$

S. N. Burmistrov and L. B. Dubovskiĭ   1835

$$J_k(E) = \int_{-(1-\tau)}^{n_{max}+\tau} dn \int_{-\infty}^{+\infty} dk_z \int_0^{\infty} k_y \, dk_y e^{2\pi i k n}$$

$$\times \frac{1}{2a} \delta\left(E - \left[\frac{k_y^2}{2m_2}(1+\xi_n) + \frac{k_z^2}{2m_3} \right] \right).$$

We shall be interested in the oscillatory part of the current density which is associated with the geometrically distinguished electron orbit corresponding to $\xi = \rho$ ($n = n_{max}$). Therefore, we shall expand γ near the point $\gamma = \frac{1}{4}$. According to Eq. (15a), this means a change from the integration variable n to ξ. Then, in the (k_y, k_z) plane it is convenient to adopt the polar coordinates:

$$k_y = [2m_2/(1+\xi)]^{1/2} p \cos\varphi, \quad k_z = (2m_3)^{1/2} p \sin\varphi.$$

Integration with respect to p removes the δ function. Integration with respect to the angle φ is carried out by the steepest-descent method collecting the main contribution near $\varphi = 0$. Integration with respect to ξ near $\xi = \rho$ gives rise to an oscillatory dependence $J_k(E)$:

$$J_k(E) = \frac{eB/c}{16\pi^3}(m_3/E)^{1/2} \exp\left(-i\frac{3\pi}{4} - i\frac{\pi k}{2} \right)$$

$$\times \rho^{-1} Q^{-1/2}(\rho) \exp\{4\pi i k m_2 E Q(\rho)\}.$$

Integration with respect to the energy E in Eq. (18) yields

$$j_v(0) = j_0 \sum_{k=1}^{\infty} \frac{\psi(k\lambda)}{k^{5/2}} \cos(k\mu/\omega_\rho - \pi k/2 + \pi/4),$$

$$\psi(z) = z/\text{sh } z, \quad \lambda = \pi T/\omega_\rho, \qquad (19)$$

$$\omega_\rho = \frac{3}{4}\frac{eB}{m_2 c}\rho^{-1/2}, \quad j_0 = \frac{3^{1/2}}{32\pi^{5/2}} e m_2^{-2}\left(\frac{m_3}{\mu}\right)^{1/2}\left(\frac{eB}{c}\right)^{5/2}\rho^{-13/4}.$$

In this case we have $(a_0/r_B)^{2/3} \ll \rho \ll 1$. The quantity μ/ω_ρ represents the number of magnetic quantum levels above the Fermi surface. The coordinate dependence of the smooth part of the current density is

$$j_v(x) = j_v(0)(1+x/l_\rho)^{-1/2},$$

$$-l_\rho(1-\Delta) < x < 0, \quad \Delta \sim (\omega_\rho/\mu)^{1/2},$$

$$l_\rho = \frac{1}{2}\rho\frac{c}{eB}(2m\mu)^{1/2} \sim \rho r_B.$$

The value of $j_v(x)$ rapidly vanishes outside a surface layer of thickness l_ρ. We shall use the fact that the current density $\mathbf{j}$ is related to the magnetic moment $\mathbf{M}$ by $\mathbf{j} = c$ curl $\mathbf{M}$ and we shall find the magnetic moment in the surface layer from Eq. (19):

$$M_z(x) = -\frac{2l_\rho}{c}(1+x/l_\rho)^{1/2}j_v(0).$$

The susceptibility $\chi = \partial M_z/\partial B_z$ can be found simply by differentiating the expression in the oscillatory vector of Eq. (19). We then find that at $T = 0$ the susceptibility is given by

$$\chi = \chi_0(\mu/\omega_\rho)^{1/2}f(\mu/\omega_\rho). \qquad (19a)$$

Here $\chi_0 \sim (v_F/c)^2$ is the Pauli susceptibility of the electron gas and f is a periodic function of the period 2π and an amplitude of the order of unity. Since $\mu/\omega_\rho \gg 1$, the susceptibility $\chi(x)$ can be considerably greater than the Pauli value, but this is true only in a thin layer of thickness l_ρ. We can readily demonstrate that not only in the case of the special orbit under discussion, but also for all the other orbits identified in Figs. 1 and 2 and characterized by energies ε which lie at the boundaries of the ranges defined by inequalities of Eq. (11), there is an oscillatory contribution to the susceptibility and its amplitude is

$$\chi \propto \chi_0(\mu/\Omega)^{1/2}. \qquad (19b)$$

Here, Ω is the cyclotron frequency of motion of an electron in a magnetic field. The above reasoning does not apply to a singularity near the bottom of a well [$\varepsilon = k_y^2/2m_2$, see Eq. (13) in the limit $\xi \to 0$] for the potential $U_B(x)$ in the case when $k_y > 0$ (Fig. 2b), which does not give rise to oscillations and—as shown below—does not contribute to the anomaly of χ. Since $\mu \gg \Omega$, it follows that the susceptibility of Eq. (19b) exceeds, like that given by Eq. (19a), very greatly the Pauli value, but it is still much less than the susceptibility in the case of the bulk de Haas–van Alphen effect[10]: $\chi_{H-A} \propto \chi_0(\mu/\Omega)^{3/2}$.

The above expressions are valid in the case of a coherent boundary in the absence of scattering. If scattering takes place near the boundary in a bicrystal, then the temperature T in Eq. (19) should be replaced with the Dingle temperature $T_D = \tau^{-1}$ (Ref. 10), where τ is the mean free time characterizing the degree of deviation of an electron from the jump-like path. An experimental investigation of the oscillations of the static quantities described by Eq. (19) can be made conveniently using a modulation method in an alternating field, when the first or second derivative of the surface impedance is found experimentally, which enhances the effect by a factor of $(\mu/\omega_\rho)^\alpha$, where α is the number of the derivative. The only restriction on the frequency of the alternating field is related to the fact that the size of the investigated bicrystal should not exceed the depth of the skin layer $\delta = c/(2\pi\omega\sigma)^{1/2}$. It should be pointed out that in this case the quantity σ differs greatly from the usual static conductivity in a magnetic field and allows for the motion along jump-like paths in a magnetic field.[14] We must bear in mind that the experimental methods give the bulk properties, i.e., that they yield $\chi_{exp} V = V(\chi_0 + \chi l_\rho/D_b)$, where D_b is the corresponding size of a bicrystal. The oscillatory effects occurring in such a system with periods characterizing the special paths of Figs. 1 and 2 and obeying the inequalities of Eq. (11) differ in respect of the period from the usual bulk de Haas–van Alphen effect. The temperature interval in which these oscillations are observed can differ from the conditions for observation of the de Haas–van Alphen effect because, for example, $\omega_\rho \gg \Omega$.

An analysis of the static susceptibility of Eq. (19) is based on the semiclassical approach. In weak fields ($\mu \gg \Omega$) when the number of the quantum levels is large and quantum oscillations take place, this approach is quite satisfactory. The wave function of the Schrödinger equation (7), expressed in terms of the parabolic cylinder functions, can be described using asymptotes of such functions, which correspond exactly to the semiclassical description. The situation

changes drastically if orbits and quantum numbers of the order of unity become important. This occurs near the bottom of the well (Fig. 2b, $k_y > 0$, near the point $\varepsilon = k_y^2/2m_2$). The quantum oscillations are then absent and we cannot use the semiclassical asymptotes of the parabolic cylinder functions. In the geometry considered here the analysis corresponds to the case of a situation near a specularly reflecting surface of a metal considered by Nedorezov (see Ref. 12 and the literature cited there), who demonstrated that a power-law anomaly of the magnetic susceptibility is not obtained if a consistent quantum-mechanical approach is adopted. We shall conclude by noting that an analogy can be drawn between the oscillations of the static quantities of Eq. (19) considered here and the de Haas–van Alphen effect under magnetic breakthrough conditions.[10,15] Magnetic breakthrough is accompanied by transitions from one band to another and this corresponds to transitions from one well to another. These transitions give rise to an additional period of the quantum oscillations of the magnetic susceptibility.

In addition to the oscillations of the static quantities of Eq. (19), transitions in an alternating field between quantum levels give rise to a resonance of the system similar to the Khaĭkin oscillations[9] of the surface impedance of a specularly reflecting metal surface considered as a function of the intensity of a static magnetic field and of the frequency of an alternating field. A detailed discussion of a resonance of this type will be given later (Sec. 6). At this stage we shall simply mention that we can distinguish it experimentally from the Khaĭkin oscillations for the specularly reflecting surface by etching this surface, which suppresses the Khaĭkin oscillations but not the resonance in question.

5. LOCALIZED STATES AT A TWINNING BOUNDARY

In the previous two sections we considered the effect occurring at the internal boundary in a bicrystal when magnetic surface levels appear in a magnetic field parallel to this boundary. A characteristic feature of these levels is that their behavior is in fact independent of the thickness L of the transition region between the two single crystals forming a bicrystal. In the present section we shall consider levels with properties governed specifically by the nature of the transition layer between these single crystals. We shall consider the case when the effective kinematic potential represents a well, as is true at a twinning boundary (Fig. 4a).

The electron energy (3) can be represented by a sum of two terms, each of which depends on just one component of the momentum:

$$E(k_y, k_z) = \varepsilon(k_y) + \frac{k_z^2}{2m_3}. \tag{20}$$

Since we are interested in the case of a twinning plane that corresponds to a symmetric potential well (Fig. 4a), we must remember that when $k_y \neq 0$ there is always at least one level in such a potential well. The number of levels increases on increase in $|k_y|$, because the potential is of kinematic origin and is proportional to k_y^2. If $|k_y|$ is sufficiently large, we can find discrete levels using semiclassical approximation:

$$\int \left[2m_{11}(x) \left(\varepsilon_n(k_y) - \frac{k_y^2}{2m_2} \frac{m_{11}(x)}{m_1} \right) \right]^{1/2} dx = \pi(n + 1/2),$$

where integration is carried out in the classically allowed region. Conversion of $\varepsilon_n(k_y)$ to the dimensionless form,

$$\varepsilon_n(k_y) = \frac{k_y^2}{2m_2}(1 + \xi_n(k_y)), \tag{21}$$

shows that the position of the discrete energy spectrum is governed by the condition

$$0 \leqslant \xi_n \leqslant \rho. \tag{21a}$$

The quantity ξ_n satisfies the equation

$$\int \{\mu(x)[\xi_n - (\mu(x) - 1)]\}^{1/2} dx = \frac{\pi}{|k_y|}(n + 1/2)(m_2/m_1)^{1/2},$$

$$\mu(x) = m_{11}(x)/m_1.$$

It follows directly from this equation that the dependence of ξ_n on k_y is not analytic at $k_y = 0$. It is convenient to discuss this in the characteristic case when the variable mass $m_{11}(x)$ differs from m_2 in a region of thickness L and is described by the expression

$$\mu(x) = m_{11}(x)/m_1 = 1 + \rho(x/L)^2, \ |x| < L, \ \rho = (m_2 - m_1)/m_1.$$

In this case the equation for ξ_n becomes

$$A(\xi_n) \equiv \xi_n \int_0^1 dy(1 - y^2)^{1/2}(1 + \xi_n y^2)^{1/2}$$

$$= \frac{\pi}{2L} \frac{(n + 1/2)}{|k_y|}(\rho m_2/m_1)^{1/2}. \tag{22}$$

In the limit of weak anisotropy ($\rho \ll 1$) the spectrum is equidistant:

$$\xi_n = 2(n + 1/2)(\rho m_2/m_1)^{1/2}/|k_y|L. \tag{22a}$$

It is clear from Eq. (21) that at low values of k_y the main term in $\varepsilon(k_y)$ is proportional to $|k_y|$. The separation between the levels is also proportional to $|k_y|$. In the opposite limiting case, typical of semimetals and semiconductors, the spectrum is nonequidistant:

$$\xi_n = \left(\frac{3\pi}{2L}\right)^{2/3}(n + 1/2)^{2/3}|k_y|^{-2/3}(\rho m_2/m_1)^{1/3}. \tag{22b}$$

In this case $\varepsilon(k_y)$ also has a singularity at $|k_y| \to 0$: $\varepsilon(k_y) \propto |k_y|^{4/3}$. The levels of Eq. (22) are similar to a discrete spectrum of an inversion layer at the contact with the semiconductor.[16] As in the case of levels in an inversion-type contact, the levels considered here behave in a special manner in the range of small momenta and this leads to singularities of the magnetic susceptibility.[17] The density of states $\nu_d(E)$ in this discrete spectrum is

$$\nu_d(E) = \frac{S}{(2\pi)^2} \sum_{n=0}^{\infty} \int_{-\infty}^{+\infty} dk_y \, dk_z \delta(E - E_n(k_y k_z)). \tag{23}$$

Summation of the states is carried out in the interval of ξ_n defined by Eq. (21a) and ξ_n is described by Eq. (22). We shall now change from summation over n to integration:

$$\nu_d(E) = \frac{S}{(2\pi)^2} \int_{-1/2}^{\infty} dn \int_{-\infty}^{+\infty} dk_y \, dk_z \delta(E - E_n(k_y k_z)).$$

The range of integration is limited to the values of ξ within

the interval $0 \leqslant \xi \leqslant \rho$. The replacement of the variables n with ξ and the subsequent integration with respect to the momenta yields the following expression for the density of states:

$$\nu_d(E) = \frac{S}{2\pi^2} L(2m_1 m_2 m_3 E)^{1/2} \alpha(\rho),$$
(23a)

$$\alpha(\rho) = \frac{4}{\pi} \rho^{-1/2} \int_0^\rho \frac{d\xi}{1+\xi} \frac{dA}{d\xi}.$$

Here, $A(\xi)$ represents the left-hand side of Eq. (22) and $\alpha(\rho)$ is a smooth function of ρ: $\alpha(\rho \to 0) = \rho^{1/2}$ and $\alpha(\infty) = 4/\pi$.

An analysis of the magnetic susceptibility of the system can be made by calculating the microscopic current of Eq. (17). In the limit of weak fields, when the thickness of the transition layer L is much less than the electron orbit radius $(L \ll r_B)$, the spectrum can be described by Eqs. (20)–(22). Retaining—as in Eq. (18)—only the smooth part of the current that does not oscillate with the coordinate, we find that

$$j_\nu(x) = 2e \frac{m_{11}(x)}{m_1 m_2} \int_0^\infty J(E) dE \Big/ \left(1 + \exp\frac{E-\mu}{T}\right),$$

$$J(E) = \int_{-\infty}^{+\infty} \frac{dk_\nu dk_z}{(2\pi)^2} \left(k_\nu - \frac{e}{c} A_\nu\right)$$

$$\times \sum_n \frac{2}{\pi} \frac{\theta(a^2-x^2)}{(a^2-x^2)^{1/2}} \delta(E - E_n(k_\nu k_z)), \quad a = L(\xi/\rho)^{1/2}.$$
(24)

The expression for $J(E)$ is calculated by analogy with the density of states $\nu_d(E)$ of Eq. (23) and, in the limit of low values of ρ, the current density can be represented by

$$j_\nu(x) = Q(x) A_\nu(x),$$
(24a)

$$Q(x) = -\frac{e^2}{m_2} \frac{8}{3\pi^3} (2m_1 m_2 m_3 \mu^3 \rho)^{1/2} \{1 - [1 - (x/L)^2]^{1/2}\}.$$

The relationship $\mathbf{j} = c\,\mathrm{curl}\,\mathbf{M}$ yields the following expression for the susceptibility:

$$\chi = -\frac{1}{c} j_\nu \Big/ \frac{\partial B}{\partial x}.$$

It follows from Eq. (24a) that the characteristic distance of a change in the magnetic induction B is L. Therefore, $\partial B / \partial x \sim B/L$ and $A_y(x) \sim BL$. Hence, the susceptibility associated with the discrete spectrum is

$$\chi_d \sim \chi_0 (L/a_0)^2.$$
(25)

Here, $\chi_0 \sim (v_F/c)^2$ is the Pauli susceptibility of the electron gas and $L/a_0 \gg 1$ is the number of discrete levels below the Fermi surface.

The quantity χ_d is the susceptibility of the discrete electron levels localized at the twinning boundary and it can exceed greatly the Pauli susceptibility and the Landau diamagnetism of the order of $(v_F/c)^2$ (Ref. 18). This enhanced value χ_d occurs in the region L. If the separation between the two twins is R_d $(R_d \gg L$, where $L \gg a_0)$, the total contribution made to the magnetization by the twins is $\chi_0 SL^3/a_0^2$, whereas the contribution of the rest of the crystal is $\chi_0 SR_d$,

where S is the surface area. All the quantities are given here per one twinning boundary. These contributions can be quite comparable. For example, if $a_0 = 4$ Å and $R_d = 200$ Å, which is true of superconducting ceramics,[5] it follows that for $L = 15$ Å we have $\chi_0 SL^3/a_0^2 \sim \chi_0 SR_d$. Like the Pauli susceptibility and the Landau diamagnetism, the susceptibility χ_d is in fact independent of temperature.

The opposite limiting case of a strong magnetic field corresponds to the limit when the radius of the electron orbit is less that the size of the transition layer between single crystals $(r_B \ll L)$. In this case the separation between the discrete levels in the transition layer is not determined by the thickness of this layer L, but by the electron orbit radius. Therefore, inside the transition layer the susceptibility is due to the de Haas–van Alphen effect in an inhomogeneous magnetic field[10] with the distribution found in the transition layer. The extremal section of the Fermi surface governing the period of quantum oscillations is determined by the positions of the crystallograph axes in the transition layer and differs from the corresponding section in the bulk of the metal. The susceptibility not only oscillates with the magnetic field, but [in contrast to Eq. (25)] it depends strongly on temperature and at $T = 0$ its value is $(v_F/c)^2(\mu/\Omega)^{3/2}$.

6. LOW-FREQUENCY RESONANCE AT A TWINNING BOUNDARY

In this section we shall consider the other alternative for a twinning boundary when a potential barrier forms at the boundary between single crystals (Fig. 4b). Then, a two-well symmetric potential appears in a magnetic field parallel to the twinning boundary (Fig. 5). The result is that the discrete levels in each of the wells becomes split and the magnitude of the splitting is an exponential function of the characteristics of the potential barrier: $\Delta \propto \Omega \exp(-D)$, where D represents the penetrability of the barrier. A resonance can occur between these closely spaced levels when an alternating electromagnetic field is applied and the resonance frequency is much less than the cyclotron frequency Ω in a magnetic field.

We shall consider our system in the case when the magnetic induction vector $\mathbf{B}$ is directed along the y axis:

$$\hat{H} = -\frac{1}{2} \frac{\partial}{\partial x} \left(\frac{1}{m_{11}(x)} \frac{\partial}{\partial x}\right)$$

$$+ \frac{1}{2} \frac{m_{11}(x)}{m_1 m_2} k_\nu^2 + \frac{1}{2m_3}\left(k_z - \frac{eB}{c} x\right)^2.$$
(26)

If $k_z = 0$, the potential $U_B(x)$ represents a symmetric two-well profile. In this case the levels in each of the wells are governed by the semiclassical condition:
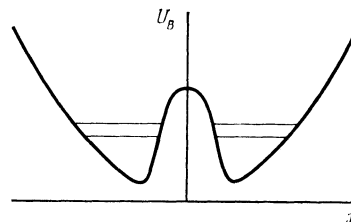

FIG. 5. Effective potential U_B in a magnetic field directed along a twinning boundary with a barrier and at right-angles to a tilt axis for electrons with the quasimomentum $k_z = 0$.

$$\int dx \left\{ 2m_{11}(x) \left[E_n - \frac{1}{2}\frac{m_{11}(x)}{m_1 m_2}k_y^2 - \frac{1}{2m_3}\left(\frac{eB}{c}x\right)^2 \right] \right\}^{1/2}$$

$$= \pi(n + \gamma_n).$$

Integration was carried out in the classically attainable region for one of the wells. In the limiting case when the electron orbit radius is much greater than the transition layer thickness ($r_B \gg L$), the positions of the levels are readily obtained in the explicit form, because they no longer depend on L:

$$E_n(k_y) = \varepsilon_n(k_y) + k_y^2/2m_1,$$
$$\varepsilon_n(k_y) = \widetilde{\Omega}(n + {}^3\!/\!_4). \tag{27}$$

The quantity $\varepsilon_n(k_y)$ satisfies the inequality

$$\varepsilon_n(k_y) < \frac{k_y^2}{2}\frac{m_1 - m_2}{m_1 m_2}, \qquad m_1 > m_2, \tag{27a}$$

where $\widetilde{\Omega} = 2\Omega$ and $\Omega = (eB/c)(m_2 m_3)^{-1/2}$ is the cyclotron frequency. Doubling of the frequency $\widetilde{\Omega}$ compared with Ω is due to the fact that an electron in a single well moves not along a whole circle, but only along half a circle. When the condition opposite to Eq. (27a) is satisfied, the classical motion occurs above the barrier between the two wells and its frequency decreases twofold:

$$E_n(k_y) = \Omega(n + {}^1\!/\!_2) + k_y^2/2m_2. \tag{27b}$$

When the condition of Eq. (27a) is satisfied so that the motion occurs in one of the wells of the two-well potential, the spectrum splits because of the presence of the second well:

$$\bar{E}_n = E_n \pm \Delta_n, \qquad \Delta_n = \frac{\widetilde{\Omega}}{2\pi}\exp\{-D(E_n)\},$$

$$D(E_n) = \int dx \left\{ 2m_{11}(x)\left[\frac{1}{2m_3}\left(\frac{eB}{c}x\right)^2 \right. \right.$$
$$\left. \left. + \frac{1}{2}\frac{m_{11}(x)}{m_1 m_2}k_y^2 - E_n \right] \right\}^{1/2}. \tag{28}$$

Integration in the expression for $D(E_n)$ is carried out in the classically forbidden region under the barrier. In the limit of a weak field we can ignore the term with the magnetic induction B in the integral and then $D(E)$ is determined only by the parameters of the transition layer L. We shall consider the following model description of $m_{11}(x)$:

$$m_{11}(x) = \begin{cases} m_1/[1 + \tilde{\rho}(x/L)^2], & |x| \leqslant L \\ m_2, & |x| \geqslant L \end{cases}, \qquad \tilde{\rho} = \frac{m_1 - m_2}{m_2} > 0.$$

In this case we have

$$D(E) = (m_1 k_y^2)^{1/2}\pi L\tilde{\rho}^{-1/2}(\tilde{\rho} - \rho_0)/[1 + (\tilde{\rho} - \rho_0)^{1/2}],$$
$$\rho_0 = 2m_1\varepsilon_n(k_y)/k_y^2 < \tilde{\rho}. \tag{28a}$$

Here, $\varepsilon_n(k_y)$ is given by Eq. (27).

These discrete levels give rise to a resonance in an alternating electromagnetic field. The expression for the current density can be deduced in the usual manner[13]:

$$j_\alpha(\mathbf{p}x) = \int dx' Q_{\alpha\beta}(\mathbf{p}, xx')\tilde{A}_\beta(\mathbf{p}x'), \tag{29}$$

where $A_\beta(\mathbf{p}x)$ is the vector potential of the alternating magnetic field. The kernel $Q_{\alpha\beta}$ consists of a regular part and a resonance correction:

$$Q_{\alpha\beta} = -\frac{Ne^2}{cm_\alpha}\delta_{\alpha\beta}\delta(x - x') + Q_{\alpha\beta}^{res},$$

$$Q_{\alpha\beta}^{res}(\mathbf{p}\omega_0, xx') \tag{29a}$$

$$= -\frac{2e^2/c}{m_\alpha m_\beta}\int\frac{dk_y\,dk_z}{(2\pi)^2}k\;k\sum_{nn'}\frac{\psi_n^2(x)\psi_{n'}^2(x')}{\omega_0 - [E_n(\mathbf{k}_+) - E_{n'}(\mathbf{k}_-)]}$$

$$\times\{f(E_n(\mathbf{k}_+) + \omega_0/2) - f(E_{n'}(\mathbf{k}_-) - \omega_0/2)\}.$$

Here, $\mathbf{k}_\pm = \mathbf{k} \pm \mathbf{p}/2$, ω_0 is the frequency of the external alternating field, and $f(E)$ is the Fermi distribution function. Since at low temperatures the distribution $f(E)$ is a step-like function near the Fermi surface, a contribution to the resonance is made only when one of the levels $E_n(\mathbf{k}_+) + \omega_0/2$ or $E_{n'}(\mathbf{k}_-) - \omega_0/2$ is occupied and the other is empty. The main contribution to the resonance appears for an extremal value of the frequency $\omega_{res}(\mathbf{p}) = E_n(\mathbf{k}_+) - E_{n'}(\mathbf{k}_-)$, which in the integrand of Eq. (29a) corresponds to the point characterized by $k_{z0} = 0$ and $k_{y0} = [2m_1(\mu - \widetilde{\Omega}(n + {}^3\!/\!_4))]^{1/2}$:

$$\omega_{res}(\mathbf{k}) = \omega_{res}(k_{y0}, 0) + \omega_{yy}(k_y - k_{y0})^2 + \omega_{zz}k_z^2,$$

where ω_{yy} and ω_{zz} are the second derivatives of the extremal frequency with respect to the momenta k_y and k_z in the twinning plane. The resonance frequency and its derivatives have the following characteristic values:

$$\omega_{res} \approx 2\Delta_n, \quad \omega_{yy} \approx \Delta_n La_0, \quad \omega_{zz} \approx \Omega a_0^2.$$

If in Eq. (29a), we used the expression for the square of the wave function

$$\psi_n^2(x) = \frac{1}{\pi}\theta(r^2 - x^2)/(r^2 - x^2)^{1/2}, \qquad r = ck_y/eB,$$

which corresponds—as everywhere in the foregoing treatment—to inclusion of only the smooth part of the wave function that does not oscillate with the coordinate, we find that the part of the kernel corresponding to the resonance is

$$Q_{yy}^{res} = \Gamma_3^{yy}\theta(r^2 - x^2)\theta(r^2 - x'^2)[(r^2 - x^2)(r^2 - x'^2)]^{1/2},$$
$$r = ck_{y0}/eB, \tag{30}$$

$$\Gamma_3^{yy} = \frac{e^2}{m_y^2}k_{y0}^2\frac{1}{2\pi^3}(|\omega_{yy}||\omega_{zz}|)^{1/2}\ln|\omega_0 - \omega_{res}(k_{y0}, 0)|/\Delta_n.$$

The above expression gives the component of the kernel Q along the y axis and this component is readily seen to be much greater than the components Q along the other coordinate axes. The logarithmic law of Eq. (30) for the resonance in the case of a general Fermi surface is enhanced to a value $|\omega_0 - \omega_{res}|^{-1/2}$ if the Fermi surface is cylindrical when Γ_3 of Eq. (30) is replaced with

$$\Gamma_2^{\alpha\beta} = \frac{e^2}{m_\alpha m_\beta}k_{y0}^2\frac{1}{4\pi^4}|\omega_{yy}|^{-1/2}|\omega_0 - \omega_{res}(k_{y0}, 0)|^{-1/2}. \tag{30a}$$

This result agrees with the size of the kernel in the case of the Khaĭkin oscillations for a cylindrical Fermi surface, when again there is a singularity of the $|\omega_0 - \omega_{res}|^{-1/2}$ type (see Ref. 19).

The ratio of the amplitude of the part of Q of Eq. (30) corresponding to the resonance of the regular part amounts to $(a_0/L)^{1/2}(\Omega/\Delta_n)^{1/2}$, and this ratio may be of the order of unity. However, the correction to the surface impedance due to the resonance is in fact always small because the twinning plane is located inside the metal where the electromagnetic field has a low amplitude due to the skin effect. Therefore, an analysis of the resonance can be made using perturbation theory. In calculations it is convenient to use the following formal procedure.[19] We shall consider a quantity

$$I = -\frac{c^2}{\omega^2}\Big[\frac{i\omega}{c}\int_{-d}^{\infty}\Big(\frac{dE_y}{dx}\Big)^2 dx + \int_{-d}^{\infty}dx\int_{-d}^{\infty}dx' E_y(x)$$

$$\times\, Q_{yy}(xx')E_y(x')\Big]\Big/ E_y^2(-d).$$

The point $(-d)$ corresponds to the position of the metal surface and the twinning plane lies at $x = 0$. Differentiating the first integral in this expression by parts and applying the Maxwell equations, we find that the quantity I is inversely proportional to surface impedance. Therefore, the correction due to the resonance given by Eq. (30) alters the surface impedance by

$$\Delta\Big(\frac{1}{\zeta}\Big) = 1/\zeta^{res} - 1/\zeta^0$$

$$= -\frac{c^2}{\omega^2}\int_{-d}^{\infty}dx\int_{-d}^{\infty}dx' E_y(x)E_y(x')Q_{yy}^{res}(xx')/E_y^2(-d).$$

Here, $\zeta^0 = (1 + i)(\omega/\delta\pi\sigma)^{1/2}$ is the value of the surface impedance in the absence of the resonance. Substituting in Eq. (31) the field distribution $E_y = E_y(-d)e^{-(x+d)/\delta}$, where $\delta^{-2} = -4\pi i\omega\sigma/c^2$, corresponding to the surface impedance in the absence of the resonance, we obtain

$$\Delta(1/\zeta) = i\frac{c}{\omega}\pi^2\Gamma_\alpha^{yy}e^{-2d/\delta}I_0^2(r/\delta), \qquad \alpha = 2, 3. \tag{32}$$

For cylindrical Fermi surface ($\alpha = 2$) the resonance correction $\Delta\zeta^{res}$ is proportional to $|\omega_0 - \omega_{res}|^{-1/2}$ and for an arbitrary Fermi surface ($\alpha = 3$) we have $\Delta\zeta^{res} \propto \ln|\omega_0 - \omega_{res}|$. In Eq. (32) the quantity $I_0(r/\delta)$ denotes a Bessel function with an imaginary argument: $I_0(x) = 1$, $x \ll 1$; $I_0(x) = e^{-x}/(2\pi x)^{1/2}$, $x \gg 1$. Therefore, $\Delta\zeta^{res}$ contains a factor $\exp(-(d-r)/\delta)$ representing the distance of the twinning plane from the surface of the investigated crystal. Consequently, an experimental study of the resonance should be made either when the twinning plane is not too far from the surface $(d - r \lesssim \delta)$, or when the twin is inclined to the surface of the crystal at a small angle θ so that a large part of the twinning plane where $(d - r) \lesssim \delta/\theta$ participates effectively in the resonance.

Equation (32) is derived on the assumption that normal skin effect conditions are satisfied: $\delta \gg l$ and $l \gg r_B$. In the case of the anomalous skin effect, when $l \gg \delta$, we again have Eq. (32), but now δ is replaced with $\delta_{eff} = (c^2/4\pi i\omega\sigma_{eff})^{1/2}$ where $\sigma_{eff} = \sigma\delta/l$ (compare Refs. 10 and 18).

This resonance is fully analogous with the Khaĭkin oscillations.[9,19] An important specific feature of the resonance is that it is located in the lower part of the spectrum which is controlled by the permeability of the potential barrier [Eq.

(28)]. In this respect it is similar to the resonance predicted in Ref. 20 for a thin film in a magnetic field when splitting of the surface levels occurs at both boundaries of the film. Experimental separation of this resonance from the Khaĭkin oscillations is possible if the surface is etched, as suggested above.

The levels and the resonant transition between them discussed in the present section depend very strongly on the geometry, because rotation of the magnetic induction vector in the plane of the bicrystal boundary makes the two-well potential asymmetric and the resonance pattern changes greatly.

7. CONCLUSIONS

It is shown here that electron surface levels appear at the twinning boundary in a bicrystal and these levels are a specific to a given type of a bicrystal. These local electron states divide naturally into two classes. The first consists of the states which are governed by the transition from one single crystal to another and depend strongly on the size of the transition layer L. These states are similar to the Tamm surface states.[21] An important property of these states is that they are of kinematic origin and are associated with the inhomogeneity of the kinetic energy in space. The second class comprises the electron states induced by a magnetic field and practically independent of the size of the transition layer L between single crystals. These states are similar to the magnetic surface states observed for a specularly reflecting metal surface.[9] The main difference is that application of a magnetic field to the boundary in a bicrystal creates a geometrically distinct electron orbit which gives rise to a new period of the quantum oscillations and this period depends on the field intensity, but is different from the period of the de Haas–van Alphen effect in the bulk of a metal. The temperature interval of possible experimental observation of such surface oscillations is different from the interval applicable to the bulk of a bicrystal.

In addition to oscillations of the static quantities, transitions between the levels in question in an alternating magnetic field give rise to the Khaĭkin oscillations of the surface impedance considered as a function of the magnetic field intensity and of the frequency of the alternating magnetic field. Experimental observation of these levels is possible not only in semimetals, as is true of a specularly reflecting crystal surface when the number of such levels is small (5–6), but also in the case of a coherent bicrystal boundary in good metals. Here the number of levels may be large. The damping of quantum oscillations and of the resonance can provide information on the degree of deviation of the bicrystal boundary from the ideal shape and on the nature of the transition layer.

The second class of surface electron states such that the separations between the levels are governed by the thickness of the transition layer L between the single crystals are the states on a twinning boundary characterized by a potential well shown in Fig. 4a. The situation of a twinning boundary with a potential barrier is intermediate between these two classes of electron states. On the one hand, the separation between the levels is governed only by the magnetic field and is practically independent of L [see Eq. (27)]. On the other hand, there is a fine structure of the levels due to their splitting by the potential barrier and the splitting is determined

by the size of the transition layer and is related to the penetrability of the barrier [see Eq. (28)]. The experimentally observed oscillatory and resonant effects can be used to identify the nature of the transition layer in a bicrystal.

Observation of these effects will provide direct information on the degree of coherence of electron motion across the internal boundary in a bicrystal. Simultaneous observation of the anomalies in the same samples[1-3] also gives a clear answer whether they are related to the coherence of the electron motion.

[1]M. S. Khaĭkin and I. N. Khlyustikov, Pis'ma Zh. Eksp. Teor. Fiz. 33, 167 (1981) [JETP Lett. 33, 158 (1981)]; A. I. Buzdin and I. N. Khlyustikov, Pis'ma Zh. Eksp. Teor. Fiz. 40, 140 (1984) [JETP 40, 893 (1984)].

[2]V. S. Bobrov and S. N. Zorin, Pis'ma Zh. Eksp. Teor. Fiz. 40, 345 (1984) [JETP 40, 1147 (1984)].

[3]L. Ya. Vinnikov, E. A. Zasavitskiĭ, and S. I. Moskvin, Zh. Eksp. Teor. Fiz. 83, 2225 (1982) [Sov. Phys. JETP 56, 1288 (1982)].

[4]B. K. Vaĭnshteĭn, Usp. Fiz. Nauk 152, 75 (1987) [Sov. Phys. Usp. 30, 393 (1987)].

[5]V. I. Simonov, V. N. Molchanov, and B. K. Vaĭnshteĭn, Pis'ma Zh. Eksp. Teor. Fiz. 46, 199 (1987) [JETP Lett. 46, 253 (1987); S. Sueno, I. Nakai, F. P. Okamura, and A. Ono, Jpn. J. Appl. Phys. Part 2 26, L842 (1987); S. Takeda and S. Hikami, Jpn. J. Appl. Phys. Part 2 26, L848 (1987).

[6]M. I. Kaganov and V. B. Fiks, Zh. Eksp. Teor. Fiz. 73, 753 (1977) [Sov. Phys. JETP 46, 393 (1977)].

[7]V. P. Naberezhnykh, V. V. Sinolitskiĭ, and É. P. Fel'dman, Zh. Eksp. Teor. Fiz. 78, 165 (1980) [Sov. Phys. JETP 51, 82 (1980)]; É. P. Fel'dman, Thesis for Degree of Doctor of Physicomathematical Sciences [in Russian], Physicotechnical Institute, Donetsk (1980).

[8]S. N. Burmistrov and L. B. Dubovskiĭ, Pis'ma Zh. Eksp. Teor. Fiz. 45, 428 (1987) [JETP Lett. 45, 547 (1987)].

[9]M. S. Khaĭkin, Usp. Fiz. Nauk 96, 409 (1968) [Sov. Phys. Usp. 11, 785 (1969)].

[10]I. M. Lifshitz, M. Ya. Azbel', and M. I. Kaganov, *Electron Theory of Metals*, Consultants Bureau, New York (1973).

[11]J. A. Appelbaum and D. R. Hamann, Phys. Rev. B 6, 2166 (1972); D. C. Langreth, Phys. Rev. B 11, 2155 (1975).

[12]S. S. Nedorezov, Zh. Eksp. Teor. Fiz. 60, 1938 (1971); 64, 624 (1973) [Sov. Phys. JETP 33, 1045 (1971); 37, 317 (1973)]; L. A. Fal'kovskiĭ, Zh. Eksp. Teor. Fiz. 58, 1830 (1970) [Sov. Phys. JETP 31, 981 (1970)].

[13]A. A. Abrikosov, L. P. Gor'kov, and I. E. Dzyaloshinskii, *Methods of Quantum Field Theory in Statistical Physics*, Prentice-Hall, Englewood Cliffs, N. J. (1963); A. A. Abrikosov, L. P. Gor'kov, and I. E. Dzyaloshinskii, *Quantum Field Theoretical Methods in Statistical Physics*, Pergamon Press, Oxford (1965).

[14]L. B. Dubovskiĭ, Zh. Eksp. Teor. Fiz. 58, 865 (1970) [Sov. Phys. JETP 31, 465 (1970)].

[15]M. I. Kaganov and A. A. Slutskiĭ, Conduction Electrons [in Russian], Nauka, Moscow (1985), p. 101.

[16]B. A. Volkov and O. A. Pankratov, Pis'ma Zh. Eksp. Teor. Fiz. 42, 145 (1985) [JETP Lett. 42, 178 (1985)].

[17]O. A. Pankratov, Phys. Lett. A 121, 360 (1987).

[18]A. A. Abrikosov, Fundamentals of the Theory of Metals [in Russian], Fizmatgiz, Moscow (1987).

[19]R. E. Prange and T. W. Nee, Phys. Rev. 168, 779 (1968).

[20]S. P. Grinberg and Y. Shapira, Solid State Commun. 56, 727 (1985).

[21]S. G. Davison and J. D. Levine, "Surface states", Solid State Phys. 25, 1 (1970); A. É. Meĭerovich and B. É. Meĭerovich, Zh. Eksp. Teor. Fiz. 93, 1461 (1987) [Sov. Phys. JETP 66, 833 (1987)].

Translated by A. Tybulewicz